Chapter 2

GEOSTATISTICAL ANALYSIS OF DOLLAR SPOT EPIDEMICS IN MICHIGAN

Introduction

Dollar spot disease of turfgrasses is caused by the pathogen, *Sclerotinia homoeocarpa* F.T. Bennett (2). The disease is common throughout the world and is destructive to both cool and warm season grasses (18, 19, 21). In North America, with the exception of the Pacific Northwest, dollar spot is the most important pathogen of most cultivated fine turfgrass species (18, 21). In Michigan, the disease is a major problem for most golf courses where the epidemic begins in June and can continue into late September. The disease can blight large areas of turf as a result of coalescing disease foci and can cause extensive damage if left untreated. Diseased turf impairs the playing surface by creating depressions that affect ball roll and areas of bare soil where weed species can encroach on the area (18, 21).

The biology of dollar spot has not been studied extensively due to the relative ease with which this disease can be controlled with fungicides. Outside of Great Britain, dollar spot has not been reported to form sexual or asexual spores (1, 13, 18, 19). Hsiang and Mahuku (11) reported that a population from Ontario exhibited DNA fingerprints that were consistent with sexual reproduction, but no fruiting bodies or spores were found. Nitrogen fertility is an important factor in the management of dollar spot (4, 14, 18, 19, 21, 25). Most reports support the view that increased fertility leads to a reduction in the severity of the disease (14, 18, 19, 21, 25). However, Couch and Bloom (4) reported that the susceptibility of

Poa pratensis was actually increased in higher fertility treatments in the greenhouse, but that the effect would be masked in the field because symptoms would not appear before the rapidly growing, infected leaf blades were mown off. Spread of the disease is widely believed to be the result of direct movement of the pathogen on infected blades during mowing operations, and human transport of infected clippings on shoes, balls, etc. (7, 18, 19, 21, 25).

Little or no research exists on inoculum sources, but some reports contend that stromatized infected tissue is the primary inoculum source for the pathogen (7, 25). Control of dollar spot via fungicide application is generally accomplished using the contact fungicide, chlorothalonil. However, the EPA has recently banned the use of this fungicide on home lawns, and future restrictions on commercial use of chlorothalonil is expected. Because the amount of fungicide available to an individual golf course is expected to be limited, it will become critical for superintendents to be able to apply chlorothalonil judiciously in areas that require treatment. Other fungicides are available for control, but fungicide resistant dollar spot populations have been reported for most of them including, the demethylation inhibiting (DMI) (8), benzimidazole (5, 23), and dicarboximide (5) fungicides.

Studying the epidemiology of a plant disease traditionally calls for the assessment of the severity or occurrence of disease over some area of interest. These data are generally collected over an area using some sampling scheme. However, traditional statistical techniques require adherence to assumptions such as the independence of samples and normality of data. It makes intuitive

sense that plants located closer in space to a diseased plant have a higher probability of becoming infected than plants located farther away. Recently, using the location of these samples in space as an additional datum has led to the description of disease epidemics over space and time using geostatistical techniques (20, 24, 26, 27).

Important epidemiological questions arise from spatially explicit descriptions of disease: Is the disease appearance clustered in space? If so, what factors contribute to this clustering? What practices might ameliorate the effects of those factors? Can we predict both when *and* where disease is going to occur so that fungicide applications can be targeted? One method available to address these questions is geostatistics. Originally developed for the study of geological phenomena, geostatistics have found wide application in a number of fields including phytopathology (20, 24, 26, 27). The primary goal of these techniques is to explain how a variate of interest (e.g. disease severity) at a location in space is correlated with all the other points where the variate has been measured (9, 10, 12, 15, 17). Further treatments allow for the prediction of the variate at unmeasured locations, and the assessment of prediction confidence. These techniques also allow for the analysis of nominal values such as genotypes or size classes in a similar manner (9, 10). Geostatistics provides a powerful set of tools that can yield insight into the dynamic nature of plant disease.

Research in plant disease epidemiology using geostatistical tools is relatively new. Geostatistics have been used to study the spatial pattern of

disease incidence and severity (20, 26) and inoculum levels (24, 27). These tools have also been used to study physico-chemical properties of soils (10), plant distributions and ecology (15, 17), and microbial distributions (20, 26, 27). Variography was used by Wollum and Cassel (26) to study the spatial variability of *Rhizobium japonicum* in soil planted with soybeans. They concluded that geostatistics were a good tool for studying the dynamics of microbial populations. Stein et. al. (20) examined the spatio-temporal development of *Peronospora parasitica* epidemics in cabbage (*Brassica oleracea*). They were able to determine that spatial variability of the fields was dependent on disease incidence. They also found spatial dependence when fields were recovering from disease. Xiao et. al. (27) studied the spatial patterns of *Verticillium dahliae* microsclerotia in the soil, and verticillium wilt in cauliflower using geostatistics. They found that the spatial structure of microsclerotia in the soil was not very strong. The structure of the microsclerotia did not play a role in the clustered appearance of disease. They attributed this to a very high amount and fairly uniform distribution of microsclerotia. They concluded other factors affect the appearance of wilt. However, they did find that the severity of the wilt was associated positively with the weak spatial pattern for the presence of microsclerotia. The information generated by a geostatistical approach to the study of plant disease epidemics allows one to develop or refine management strategies, and help to determine the contributing factors that deserve further study. Ultimately, this information can be used to design models that can be used

to predict the occurrence of plant disease, helping to minimize pesticide applications, or make cultural practices more effective.

We had 3 objectives: 1) to observe dollar spot epidemics and determine if disease occurrence has a spatial structure, 2) if a spatial structure is present, determine the geostatistical parameters associated with the spatial structuring, 3) Determine if the spatial structure changes during an epidemic, or over seasons.

Materials and Methods

Sampling. The study site was established at the Robert Hancock Turfgrass Research Center on a 9.1 m X 18.3 m area of creeping bentgrass (*Agrostis palustris* Huds.) and annual bluegrass (*Poa annua* L.). The study site received no fungicide applications from 2000-2002. The study site was divided into 200 0.3 m^2 areas on a regular grid at 0.9 m intervals in 2000. In 2001, 23 additional 0.30 m^2 areas were established at random locations within the study site, and all 223 areas were subdivided into four 0.15 m subareas (Fig. 1). These additional locations were added and all areas subdivided to increase the number of data pairs at small lag distances. Each subarea's x,y coordinates were recorded using its center. A 0.3 m^2 wooden frame that was divided into quadrants was used to delineate the subareas. Two points at each sampling location were marked with marking paint in order to place the frame at the same location at each sample time. Isolates were also collected from an arbitrarily selected dollar spot at each location in July 2000 and the vegetative compatibility group (VCG) for each isolate was determined in order to assess if clustering was present in VCGs (Appendix 1).

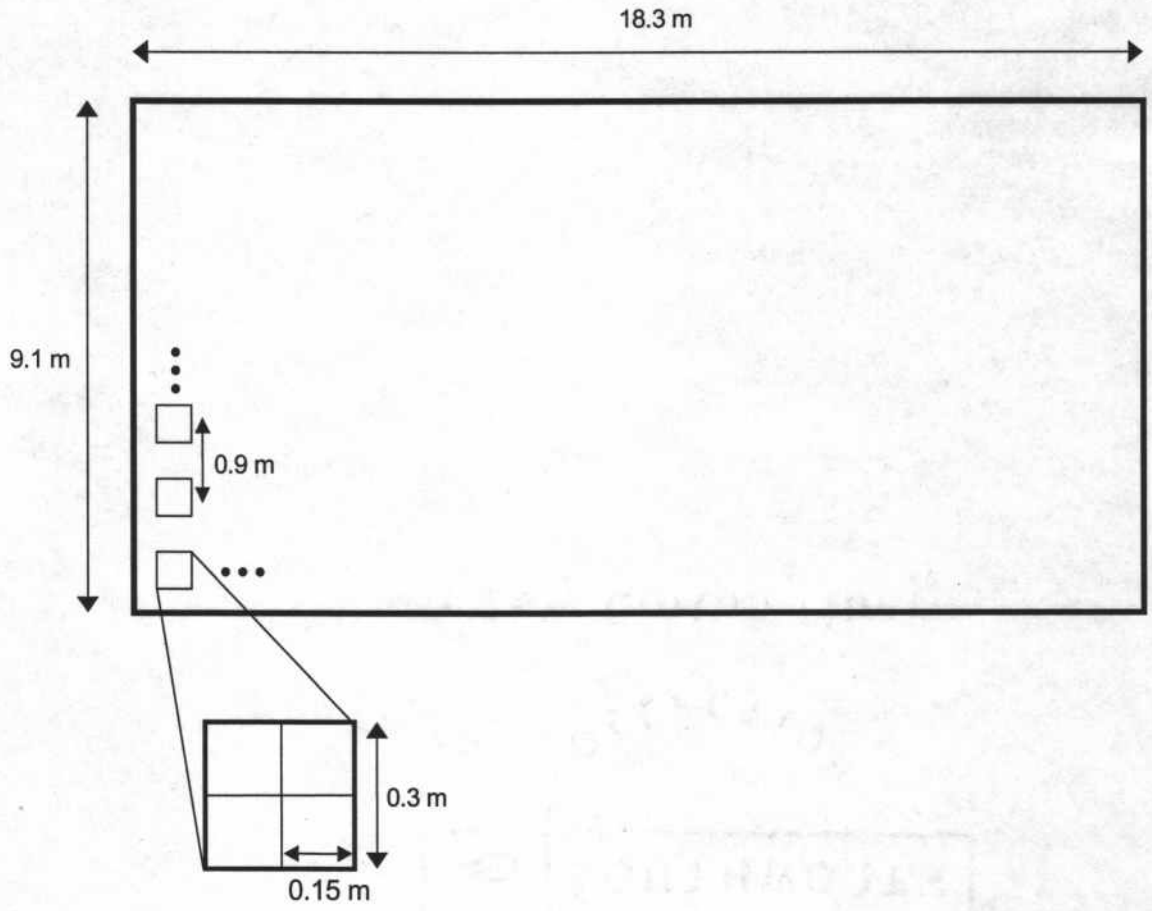

Figure 1. Schematic layout of study area at the Robert Hancock Turfgrass Research Center (E. Lansing, MI) showing overall arrangement of sampling locations.

Data Collection. Dollar spot foci were counted three times per week in 2000 and twice per week in 2001 and 2002 from each of the locations in the study area. Foci were counted when they reached a size large enough to observe. This helped to minimize the possibility of accidentally counting an area that was not a true dollar spot. Counting of the study area was stopped in each year when disease became prevalent enough in a location that there were too many disease foci to count accurately.

Geostatistical analysis. Spatial continuity was measured using the variogram, that describes how a variate changes over space. Intrinsic to geostatistical analysis is the hypothesis that the expectation of differences between any pair of points depends solely on the distance (h) between the points (6, 9, 12). Therefore, to estimate the variogram from disease incidence data with the intrinsic hypothesis in mind;

$$\gamma\,(\mathrm{h}) = \frac{1}{2N(h)} \sum_{(i,j)|h_{ij}=h} (v_i - v_j)^2$$

where γ is the semivariance, h is the average separation distance between pairs of points, N is the number of data pairs, and v_i and v_j are the ith and jth data values at separation distance h. This results in estimates of semivariance (γ) that are plotted as a function of separation distance (h). Once a variogram is calculated, a model that fits the observed data can be fit to the experimental data. A variogram model defines three key parameters: nugget, sill, and range. The nugget is the result of the discontinuity that occurs when the semivariance, which is defined to be 0 when lag distance, h=0, jumps to some value > 0 at a

very small distance away. The nugget is the result of a combination of sources of variation including experimental error and short-scale variability (9, 12). Generally, as the distance between pairs of points increases, the semivariance will also increase. Therefore as pairs of points are separated by larger distances they become less correlated. However, at some separation distance between pairs the semivariance will reach a plateau where increases in separation distance do not result in a change in the semivariance. This distance where semivariance reaches a plateau is the range, and is also the boundary between spatially dependent and spatially independent variation. The third parameter calculated for a variogram model is the sill. It is defined as the semivariance value reached at the range. If the sampling design has accounted for most of the variation in the system, then the sill value is often very similar to the overall sample variance (s^2). The total variance can be ascribed to three catagories: nugget (Co), structural or spatial variance (C), and sill variance ($Co+C$). The proportion of the total variance that is accounted for by structural variance, or the proportion of structural variance, can be calculated by, $C/Co+C$, and is often expressed as a percentage of the total variance that is spatially structured. When this value approaches 1, a large proportion of the total sample variance is spatially dependent. When the value approaches 0, spatial dependence is low. If the sill value ($Co+C$) is not similar to the total sample variance (s^2), this indicates that there may be further structure at scales larger than those sampled.

Variograms were calculated using the windows interface WinGSLIB (Statios, LLC., San Francisco, CA) for the geostatistical software package,

GSLIB (version 9) (6). The choice of the number of lags, lag interval, and lag tolerance were defined iteratively based on the number, interval and tolerance for lags that yielded a smooth, well-behaved variogram. Ultimately, 15 lags with a 0.61 m lag interval, and 0.30 m lag tolerance were the parameters that gave the most well-behaved result for all three years. The experimental variograms were then modeled using the geostatistical software package, GS+ version 3.0 (Gamma Design Software, Plainwell, MI). The GS+ software package allows one to automatically fit models to the experimental variogram, and then chooses the best fit based on the model with the smallest unweighted least squares value. Any additional changes that were necessary were made by hand to the initial fit provided by the program. The experimental variograms used for modeling were generated in the GS+ program using a 12.2 m lag distance and 1.5 m lag interval as parameters for 2000, and a 6.1 m lag distance and .61 m lag interval for 2001 and 2002. These distances were chosen to avoid over-fitting the models to the increasing semivariance values at larger lag distances seen in the experimental variograms shown in Figure 3.

Results

Sampling and *Data Collection*. Disease was observed and the number of dollar spot foci counted at each location until August 25th in 2000, September 9th in 2001, and September 13th in 2002. Total disease progress curves for each of the three years appear in Figure 2. The epidemic in 2002 was the most severe followed closely by the epidemic in 2000. The epidemic in 2001 was much less severe than either 2000 or 2002. The total disease progress curves for all three

years were similar in shape. Each progress curve had an early season outbreak that was not as severe as the late season outbreak that began in early August and continued into September.

Geostatistical analysis. Variograms were calculated for each date disease counts were taken in 2000-2002. Nine variograms, each representing a variogram from the early, middle, and late phases of the epidemic for each year are shown in Figure 3. The remaining variograms from other sample dates are presented in Appendix 2. Anisotropy was examined at several dates and no anisotropic trends were apparent (Data not shown). The variograms in all three years show clear spatial structuring that occurs at smaller lag distances (<0.9 m), particularly as disease incidence increases over time. Throughout 2001 and 2002 the model that best fit the data was an exponential model (Table 1). In 2000, the first three dates showed a nugget effect indicating no spatial structuring, and then for the remainder of the season both spherical and exponential models were defined. The proportion of structural variance ($C/Co+C$) was about 0.5 for 2000 and about 0.6 for both 2001 and 2002 (Table 2). This value means that about 50% of the total variation in 2000 and about 60% of the total variation in 2001 and 2002 is spatially structured. The range parameter that was calculated for each variogram model in 2000 had larger values and a wider range of variation as compared to the smaller and less variable range parameters calculated in 2001 and 2002.

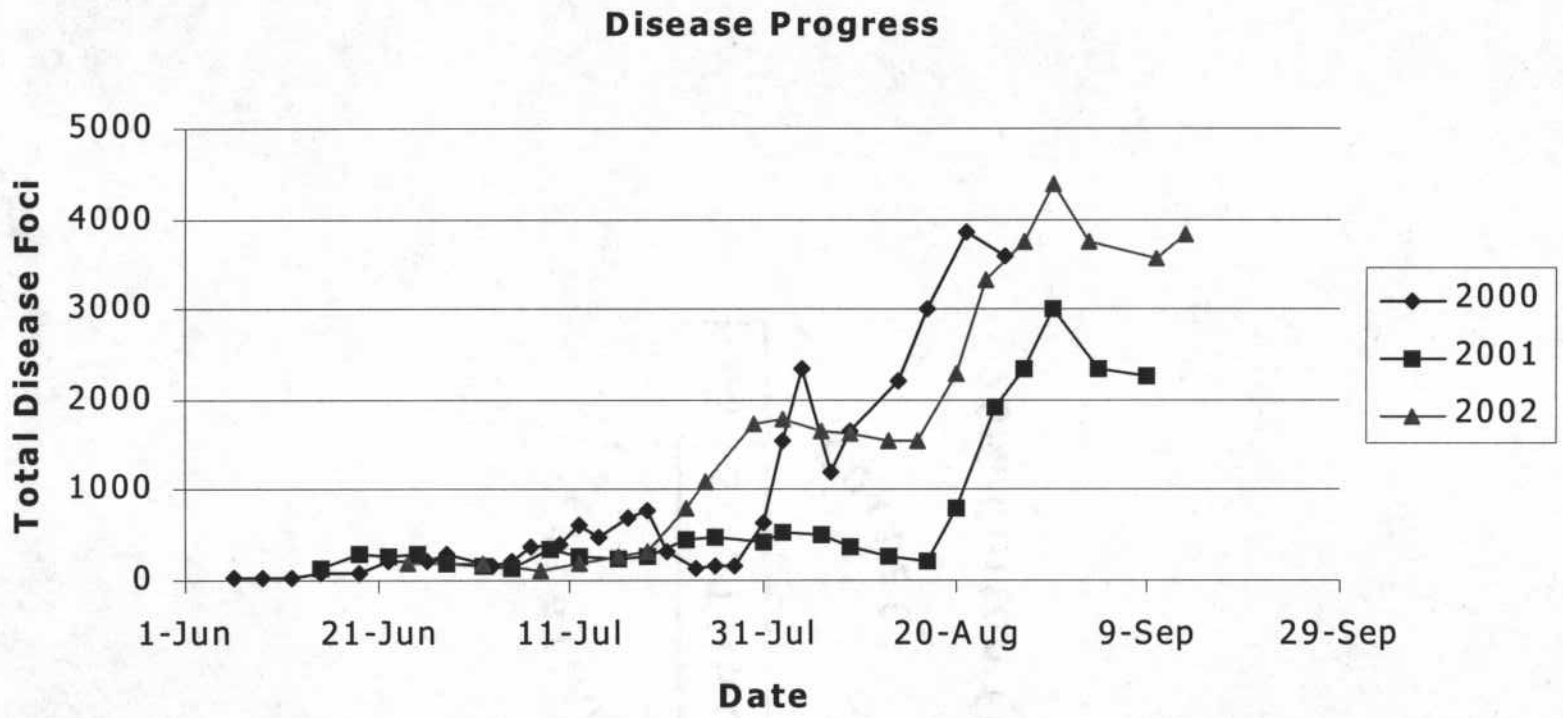

Figure 2- Graph comparing total disease progress from 2000-2002 as measured by counts of total disease foci in all sample locations.

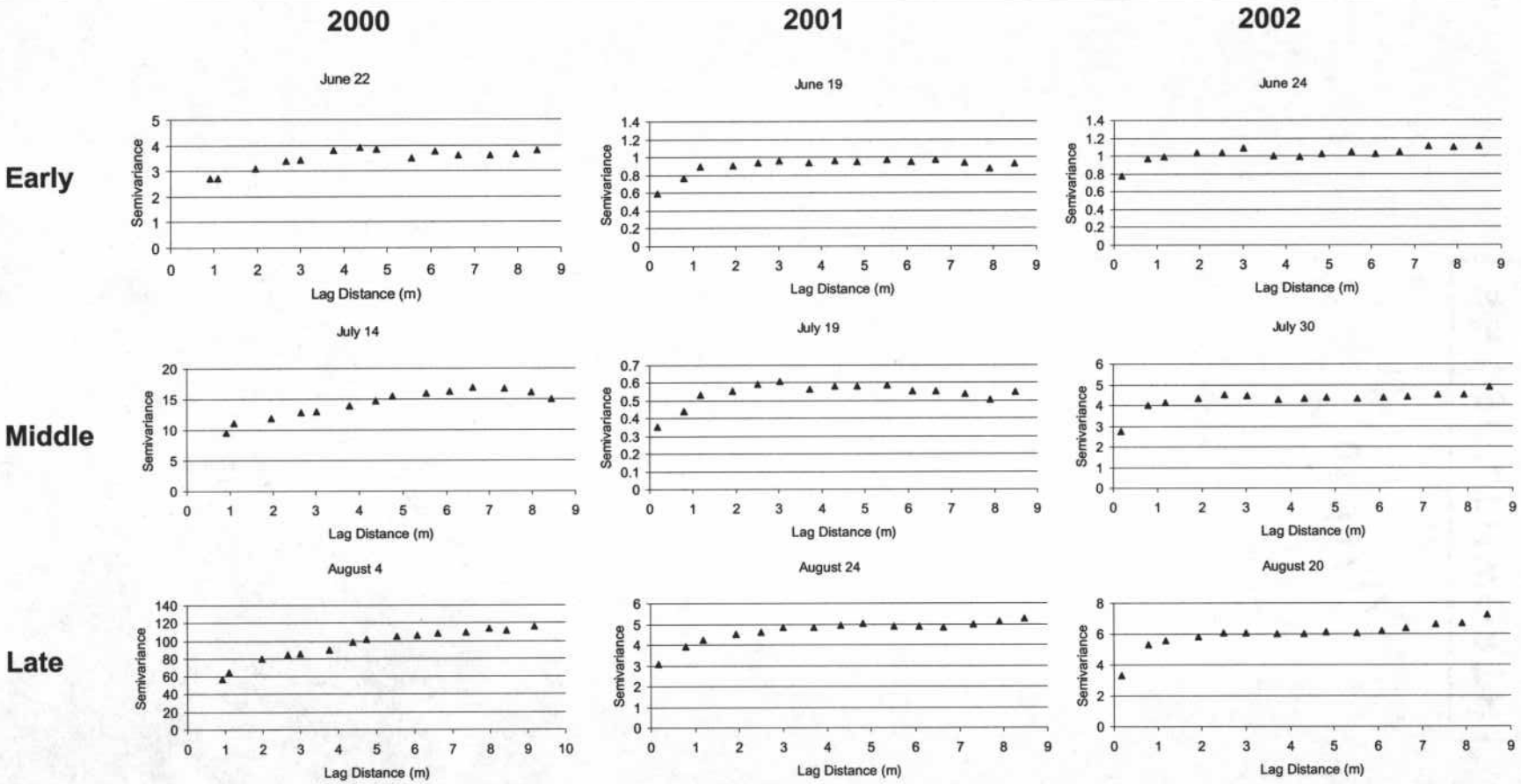

Figure 3. Experimental variograms from 2000-2002 measuring spatial dependence from the early, middle, and late phases of the dollar spot epidemic.

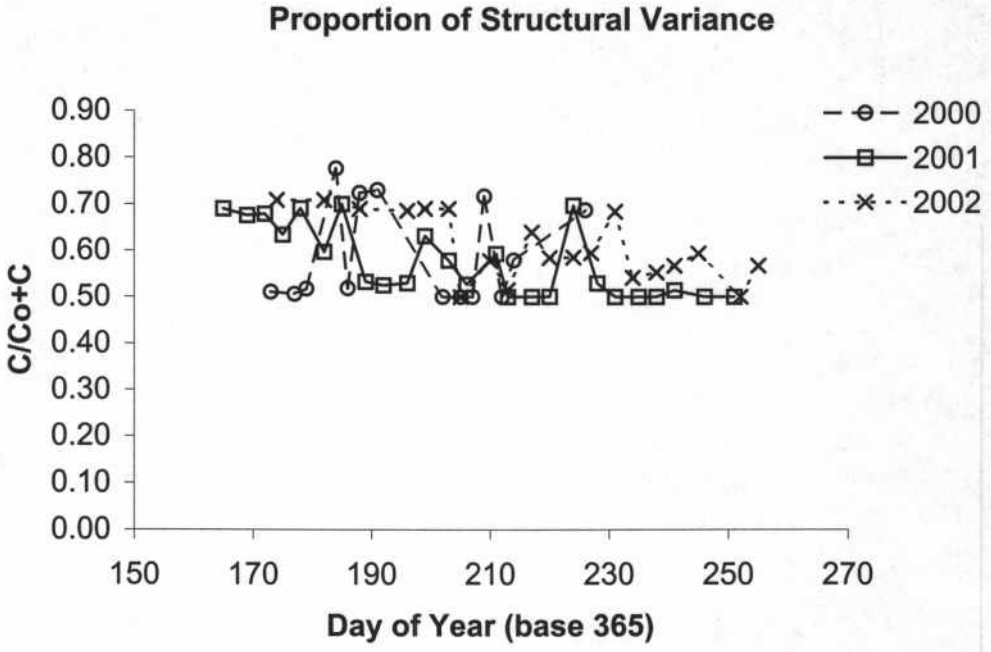

Figure 4. Graph showing the proportion of structural variance (C/Co+C) over time for exponential variogram models from 2000-2002.

Year	Date	Model Type	Nugget (*Co*)	Sill (*Co*+*C*)	Range (3a)	r^2	RSS
2000	22-Jun	Exponential	1.96	4.004	21.72	0.87	0.209
2000	14-Jul	Exponential	7.38	16.29	21.30	0.885	3.121
2000	4-Aug	Exponential	33.9	109.9	20.37	0.916	169.8
2001	19-Jun	Exponential	0.176	0.543	4.39	0.988	6.04E-04
2001	19-Jul	Exponential	0.215	0.584	5.68	0.962	2.05E-03
2001	24-Aug	Exponential	2.474	4.949	8.78	0.977	0.0777
2002	24-Jun	Exponential	0.11	0.378	2.25	0.754	2.52E-03
2002	30-Jul	Exponential	1.841	4.363	4.01	0.964	0.0642
2002	20-Aug	Exponential	1.91	6.051	4.42	0.991	0.0458

Table 1. Variogram model parameters (nugget, sill, range), goodness of fit (r^2), and residual sum of squares (RSS) for the nine experimental variograms shown in Figure 3. (Range for exponential model is defined as 3a due to the asymptotic behavior of the model).

Year	Date	Nugget (Co)	Sill (Co+C)	Proportion of Structural Variance (C/Co+C)
2000	6-Jun	0.082	0.082	0.00
2000	9-Jun	0.135	0.135	0.00
2000	12-Jun	0.111	0.111	0.00
2000	15-Jun	0.633	1.207	0.48
2000	19-Jun	0.629	0.908	0.31
2000	22-Jun	1.96	4.004	0.51
2000	26-Jun	2.182	4.418	0.51
2000	28-Jun	3.41	7.068	0.52
2000	3-Jul	0.812	3.636	0.78
2000	5-Jul	1.873	3.889	0.52
2000	7-Jul	3.6	13.05	0.72
2000	10-Jul	3.56	13.2	0.73
2000	12-Jul	11.96	23.93	0.50
2000	14-Jul	8.08	16.17	0.50
2000	17-Jul	12.33	24.67	0.50
2000	19-Jul	16.86	33.73	0.50
2000	21-Jul	4.04	8.081	0.50
2000	24-Jul	1.766	3.533	0.50
2000	26-Jul	2.097	4.195	0.50
2000	28-Jul	0.913	3.23	0.72
2000	31-Jul	10.62	21.25	0.50
2000	2-Aug	26.9	63.92	0.58
2000	4-Aug	51.9	108.7	0.52
2000	7-Aug	17.92	46.7	0.62
2000	9-Aug	33.7	72.28	0.53
2000	14-Aug	35	112.12	0.69
2000	17-Aug	46.9	130.8	0.64
2000	21-Aug	54.3	171.4	0.68
2000	25-Aug	45.9	161.7	0.72
			Mean	0.51

Year	Date	Nugget (Co)	Sill (Co+C)	Proportion of Structural Variance (C/Co+C)
2001	15-Jun	0.075	0.242	0.69
2001	19-Jun	0.176	0.543	0.68
2001	22-Jun	0.162	0.505	0.68
2001	25-Jun	0.165	0.451	0.63
2001	28-Jun	0.088	0.285	0.69
2001	2-Jul	0.083	0.206	0.60
2001	5-Jul	0.056	0.187	0.70
2001	9-Jul	0.308	0.659	0.53
2001	12-Jul	0.239	0.503	0.52
2001	16-Jul	0.236	0.502	0.53
2001	19-Jul	0.215	0.584	0.63
2001	23-Jul	0.374	0.888	0.58
2001	26-Jul	0.422	0.892	0.53
2001	31-Jul	0.343	0.844	0.59
2001	2-Aug	0.549	1.099	0.50
2001	6-Aug	0.487	0.975	0.50
2001	9-Aug	0.357	0.715	0.50
2001	13-Aug	0.116	0.384	0.70
2001	17-Aug	0.184	0.391	0.53
2001	20-Aug	0.964	1.929	0.50
2001	24-Aug	2.474	4.949	0.50
2001	27-Aug	2.049	4.099	0.50
2001	30-Aug	2.753	5.669	0.51
2001	4-Sep	1.725	3.451	0.50
2001	9-Sep	1.542	3.085	0.50
			Mean	0.57

Year	Date	Nugget (Co)	Sill (Co+C)	Proportion of Structural Variance (C/Co+C)
2002	24-Jun	0.11	0.378	0.71
2002	2-Jul	0.11	0.378	0.71
2002	8-Jul	0.062	0.2	0.69
2002	12-Jul	0.41	0.41	0.00
2002	16-Jul	0.129	0.411	0.69
2002	19-Jul	0.156	0.504	0.69
2002	23-Jul	0.521	1.683	0.69
2002	25-Jul	1.19	2.381	0.50
2002	30-Jul	1.841	4.363	0.58
2002	2-Aug	2.126	4.386	0.52
2002	6-Aug	1.569	4.355	0.64
2002	9-Aug	1.79	4.308	0.58
2002	13-Aug	1.803	4.348	0.59
2002	16-Aug	1.742	4.299	0.59
2002	20-Aug	1.91	6.051	0.68
2002	23-Aug	3.86	8.413	0.54
2002	27-Aug	3.96	8.855	0.55
2002	30-Aug	4.22	9.75	0.57
2002	3-Sep	3.37	8.293	0.59
2002	10-Sep	3.44	6.881	0.50
2002	13-Sep	3.47	8.019	0.57
			Mean	0.58

Table 2- Variogram model parameters for each rating date in 2000-2002 showing nugget, sill, and proportion of structural variance values.

Discussion

Although the total disease severity during the epidemics in each of the three years was different, there were also several similarities between the epidemics. First, the disease progress curves were similar in shape (Fig. 2). All three progress curves showed that dollar spot first appears in early to mid June with a minor outbreak and then becomes much more severe during the months of August and September. Our data agree with those of other researchers that have shown the later season phase of the epidemic is most damaging to a turf area (7, 16, 18, 21). Disease progress was similar in each year despite differences in disease severity indicating that environmental parameters play a large role in the overall severity and timing of dollar spot outbreaks. In all three years dollar spot was observed to decrease in presence during July, presumably because of the hot, humid growing conditions present during that time. These results support the view that environmental parameters are primarily responsible for disease appearance and resulting overall severity.

The experimental variograms that were calculated for each date were also similar over time. Once a variogram is calculated for each date in the study, a model is calculated that fits the observed data. One reason to fit models to the data is so that the key model parameters the nugget, range, and sill, can be compared to observe how they change over time. The sampling design determines the smallest scale at which spatial relationships can be resolved. In 2000 the design consisted of 200 0.3 m^2 areas spaced on 0.9 m centers. The limitations of this design is that the smallest lag interval for the calculated

variogram was 0.9 m, and there was no information about the disease at smaller scales. If spatial dependence exists at a scale smaller than the smallest sampled interval, then it would become a part of the nugget variance and would not be accounted for in the variogram. In 2000, the calculated variograms displayed spatial dependence, and about 50% of the total variation was spatially structured (Table 2). In 2001 and 2002 23 additional areas were added randomly to the study site, and the 0.3 m^2 areas were subdivided into four 0.15 m^2 subareas to protect against the possible problem of the scale of spatial dependence. Increasing the resolution of the sampling design increased the information about small-scale variability. As the smallest sampling interval was 0.15 m, the addition of the random locations was important to be able to evaluate lag distances between 0.15 m and 0.9 m. These changes in the sampling design resulted in a gain of information as reflected by a 10% increase in the proportion of structural variance from 50% in 2000 to 60% in 2001 and 2002 (Table 2). This increase in spatial resolution at the smaller scales is why there is a much stronger spatial dependence observed for the 2001 and 2002 data as compared to the 2000 data. Based on the experimental variograms calculated for all three years we conclude that dollar spot incidence is spatially correlated in our study area, and that the spatial correlation is present on a small scale. Other locations should be included in future studies to determine if dollar spot incidence at other locations is similarly spatially correlated.

Interestingly, the nugget and sill values for variogram models from each date scale with one another indicating that the spatial structure is relatively stable

over time. The stability of this relationship can also be seen in the stability of the proportion of structural variance (*C/Co+C*) over time (Figure 4). The range parameter is also relatively stable further confirming a structure that is stable and relatively constant over time. While the range did fluctuate in 2000, the smallest lag interval was only 0.91 m, and these fluctuations could be a function of the lack of small-scale sampling. The higher resolution in 2001 and 2002 decreased the fluctuations in the range parameter where the overall change in the range from low to high in both years was between two and three meters. Exponential variogram models were defined in all three years. These results clearly show that as disease intensity increases over a season, the spatial structure that is present is stable and doesn't change much over time.

One possible explanation for the observed spatial structure is that areas with more disease increase at the same relative amount as areas with less disease. If this were not the case, then one would expect the spatial structure, as measured by the proportion of structural variance (*C/Co+C*), to change as disease increased over the season. However, the structure that was observed remained stable over the season. The distance between areas with similar disease intensities (i.e. range) also remains relatively stable over time indicating that these areas are not shifting within an epidemic or among epidemics. Because one would expect different locations to behave differently as a result of either micro- or macroclimatic changes that occur over an epidemic, these results support the view that environmental parameters are not a major factor in the spatial structuring at the scales observed.

The literature provides much speculation on the mode of spread for this non-spore forming pathogen (7, 11, 18, 25). These reports range from the movement of mycelial fragments on diseased tissue via human and mechanical transport (7, 18, 25) to the production of an undiscovered spore that is produced (11). Data from this study disagree with both of these possibilities. If the pathogen were transferred via mechanical means, then one would expect the spatial structure of disease incidence to change over time because mycelial fragments would be distributed over the area via regular, uniform mowing practices. If the pathogen was transferred via human means, then the spatial structure should be indicative of a pattern similar to a pattern of movement over the area by people. If this pathogen produced some unknown spore, then one would expect that the dispersal of such a spore would occur such that the spatial structure of the disease would change with the release of spores. However, none of these possible outcomes were observed in this study. Rather, our results indicate that the primary factor governing the spatial structure is one that doesn't move in space and whose spatial structure is relatively constant regardless of the intensity of disease.

One hypothesis that would fit these data is that the host and/or pathogen are important in the spatial structuring. The predominant grasses found on golf course putting surfaces are creeping bentgrass (*A. palustris*) and annual bluegrass (*P. annua*). Both of these grasses are non-uniform in their susceptibilities to *S. homoeocarpa* (3, 22). The breeding strategy employed for creeping bentgrass results in the production of a synthetic cultivar, meaning that

each seed is genetically distinct. This results in a range of variation in susceptibility/resistance to dollar spot. Annual bluegrass is a non-cultivated grass that invades putting surfaces as a weed, and also is known to be genetically variable (21). The area we studied was at least 10 years of age and was a mixed sward of creeping bentgrass and annual bluegrass. Over time the competitiveness of each seedling would govern those genotypes of grasses found in a site. These successful genotypes would then be more or less susceptible to dollar spot, and this would be observed as a mosaic of disease incidence with a spatial structure corresponding to the spatial structure of the grasses. This hypothesis would also predict that the inoculum density of the pathogen would also follow this spatial structure because areas with previous higher disease incidence would produce more infested tissue, which is believed to be the primary inoculum source for dollar spot.

Overall, these data support the view that there is a relatively stable spatial structure governing disease incidence that is unaffected by disease severity. Furthermore, the results support a theoretical model that the host and pathogen are involved in the observed spatial structure over the scales assessed by this study, and that environmental parameters appear to be most important in overall disease severity and timing of disease outbreaks.

Future research in this area should include the evaluation of other locations to determine if the observed spatial structure is ubiquitous, and the testing of the theoretical models posed by this research to confirm or exclude factors associated with the spatial structuring of dollar spot incidence. These

research areas would provide the information that is needed to begin developing predictive models that can predict the incidence and location of dollar spot based on a knowledge of the environmental and geospatial parameters that govern where and when dollar spot occurs. Once predictive models become available it would then be possible to implement precision fungicide applications for the control of this disease.

Literature Cited

1. Baldwin, N.A. and Newell, A.J. 1992. Field production of fertile apothecia by *Sclerotinia homeocarpa* in *Festuca* turf. J. Sports Turf Res. Inst. 68: 73-76.

2. Bennett, F.T. 1937. Dollar spot of turf and its causal organism *Sclerotinia homoeocarpa* n. sp. Ann. Appl. Biol. 24: 236-257.

3. Cole, H., Duich, J.M., Massie, L.B., and Barber, W.D. 1969. Influence of fungus isolate and grass variety on *Sclerotinia* dollar spot development. Crop Science 9: 567-570.

4. Couch, H.B., and Bloom, J.R. 1960. Influence of turfgrasses. II. Effect of nutrition, pH, and soil moisture on *Sclerotinia* dollar spot. Phytopathology 50: 761-763.

5. Detweiler, A.R., Vargas, J.M., Jr., and Danneberger, T.K. 1983. Resistance of *Sclerotinia homoeocarpa* to iprodione and benomyl. Plant Dis. 67: 627-630.

6. Deutsch C.V., and Journel, A.G. 1998. GSLIB: Geostatistical Software Library and User's Guide 2nd Edition. Oxford University Press, New York.

7. Fenstermacher, J.M. 1980. Certain features of dollar spot disease and its causal organism *Sclerotinia homoeocarpa*. In: Advances in Turfgrass Pathology. Eds. P.O. Larsen and B.G. Joyner, Harcourt, Brace, Jovanovich, Duluth, MN, pp. 49-53.

8. Golembiewski, R.C., Vargas, J.M.,Jr., Jones, A.L., and Detweiler, A.R. 1995. Detection of demethylation inhibitor (DMI) resistance in *Sclerotinia homoeocarpa* populations. Plant Dis. 79: 491-493.

9. Goovaerts, P. 1997. Geostatistics for Natural Resources Evaluation. Oxford University Press, New York.

10. Goovaerts, P. 1998. Geostatistical tools for characterizing the spatial variability of microbiological and physico-chemical soil properties. Biol. Fertil. Soils 27, 315-334.

11. Hsiang, T., and Mahuku, G.S. 1998. Genetic variation within and between southern Ontario populations of *Sclerotinia homeocarpa*. Plant Pathology 48: 83-94.

12. Isaaks, E.H., and Srivastava, R.M. 1989. An Introduction to Applied Geostatistics. Oxford University Press, New York.

13. Jackson, N. 1973. Apothecial production in *Sclerotinia homeocarpa* F.T. Bennett. J. Sports Turf Res. Inst. 49: 58-63.

14. Markland, R.E., Roberts, E.C., and Frederick, L.R. 1969. Influence of nitrogen fertilizers on Washington creeping bentgrass, *Agrostis palustris* Huds. II. Incidence of dollar spot, *Sclerotinia homoeocarpa* infection. Agron. J. 61: 701-705.

15. Oliver, M.A. and Webster, R. 1986. Combining nested and linear sampling for determining the scale and form of spatial variation of regionalized variables. Geographical Analysis 18: 227-242.

16. Powell, J.F., and Vargas, J.M., Jr. 2001. Vegetative compatibility and seasonal variation among isolates of *Sclerotinia homoeocarpa*. Plant Dis. 85: 377-381.

17. Rossi, R.E., Mulla, D. J., Journel, A. G., and Franz, E. H. 1992. Geostatistical tools for modeling and interpreting ecological spatial dependence. Ecological Monographs 62: 279-314.

18. Smith, J.D., Jackson, N., and Woolhouse, A.R. 1989. Fungal Diseases of Amenity Turf Grasses. E. and F. Spon, New York.

19. Smiley, R.W. 1992. Compedium of Turfgrass Diseases 2nd Edition. American Phytopathology Society Press, St. Paul, MN.

20. Stein, A., Kocks, C.G., Zadoks, J.C., Frinking, H.D., Ruissen, M.A., and Myers D.E. 1994. A geostatical analysis of the spatio-temporal development of downy mildew epidemics in cabbage. Phytopathology 84: 1227-1239.

21. Vargas, J.M., Jr., 1994. Management of Turfgrass Diseases. Lewis Publishers, Ann Arbor, MI.

22. Vincelli, P., and Doney J.C.,Jr. 1997. Variation among creeping bentgrass cultivars in recovery from epidemics of dollar spot. Plant Dis. 81: 99-102.

23. Warren, C.G., Sanders, P., and Cole, H. 1974. *Sclerotinia homoeocarpa* tolerance to benzimidazole configuration fungicides. Phytopathology 64: 1139-1142.

24. Webster, R., and Boag B. 1992. Geostatistical analysis of cyst nematodes in soil. Journal of Social Science 43: 583-595.

25. Williams, D.W., Powell, A.J., Jr., Vincelli, P., and Dougherty, C.T. 1996. Dollar spot on bentgrass influenced by displacement of leaf surface moisture, nitrogen, and clipping removal. Crop Sci. 36: 1304-1309.

26. Wollum, A.G.,II, and Cassel, D.K. 1984. Spatial variability of *Rhizobium japonicum* in two North Carolina soils. Soil Science Soc. Am. J. 48, 1082-1086.

27. Xiao, C. L., J. J. Hao, and K. V. Subbarao. 1997. Spatial patterns of microsclerotinia of *Verticillium dahliae* in soil and verticillium wilt of cauliflower. Phytopathology 87 (3), 325-331.